Inorganic Chemistry

Article

pubs.acs.org/IC

Two Three-Dimensional Lanthanide Frameworks Exhibiting Luminescence Increases upon Dehydration and Novel Water Layer Involving in Situ Decarboxylation

Ai-Hong Yang,[‡] Ji-Yong Zou,[†] Wen-Min Wang,[†] Xue-Ying Shi,[†] Hong-Ling Gao,[†] Jian-Zhong Cui,*[,†] and Bin Zhao*[,§]

[†]Department of Chemistry, School of Science, Tianjin University and Collaborative Innovation Center of Chemical Science and Engineering (Tianjin), Tianjin 300072, People's Republic of China

[‡]Tianjin Key Laboratory of Chemistry and Analysis of Chinese Materia Medica, College of Chinese Materia Medica, Tianjin University of Traditional Chinese Medicine, Tianjin 300193, People's Republic of China

[§]College of Chemistry, Nankai University, Tianjin 300071, People's Republic of China

Supporting Information

ABSTRACT: Two three-dimensional polymeric Tb(III) and Yb(III) frameworks, namely, $\{[Tb_3(Hptc)(ptc)(pdc)(H_2O)_6]\cdot 2H_2O\}_n$ (**1**) and $\{[Yb_2(ptc)(ox)(H_2O)_5]\cdot 7H_2O\}_n$ (**2**) (H_4ptc = pyridine-2,3,5,6-tetracarboxylic acid, H_2pdc = pyridine-3,5-dicarboxylic acid, ox = oxalate), have been synthesized by a hydrothermal method and characterized by infrared spectra, elemental analysis, powder X-ray diffraction, thermogravimetric analysis, and single-crystal X-ray diffraction. Framework **1** shows an interesting three-dimensional (8,8)-connected net with a Schläfli symbol of $(3^3\cdot4^{18}\cdot5^5\cdot6^2)_2(3^6\cdot4^{14}\cdot5^7\cdot6)$, while **2** exhibits an unusual (4,8)-connected **sqc21** net with a Schläfli symbol of $(3^2\cdot4^2\cdot5^2)(3^4\cdot4^8\cdot5^{12}\cdot6^4)$. Luminescence studies of **1** reveal that the luminescence intensity increases when the framework is dehydrated.

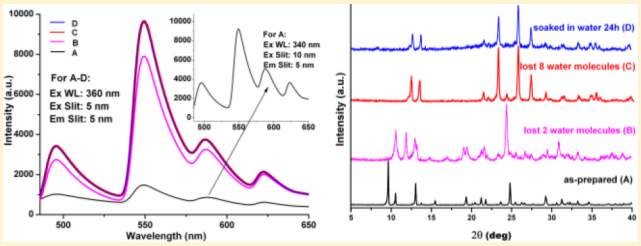

INTRODUCTION

Hydro(solvo)thermal synthesis has been a promising technique in preparing hybrid materials with novel structures and special properties.[1] However, unexpected results may occur because many factors have been found to have a significant influence on the products. Decarboxylation can occur under hydro(solvo)-thermal conditions,[2] which can proceed via C−C bond cleavage.[3] Although decarboxylation reactions will increase the difficulty of the syntheses of compounds with required structures, they generate some novel compounds containing interesting organic species that are difficult to obtain by routine synthetic methods.[4] There have been many reports that transition metals such as Cu(II), Mn(II), Zn(II), and Cd(II) ions play a unique catalytic role in decarboxylation reactions.[2,5−14] Few reports describe decarboxylation reactions involving lanthanide ions.[15,16] In such reactions, some multi-carboxylic acid ligands lost their partial carboxyl groups through cleavage of the C−C bond and release of CO_2 molecules, and then the decarboxylation products coordinated metal ions.[15] In other cases,[16] oxalate can be obtained in decarboxylation through the process that includes the anionic $^{\cdot}CO_2^-$ radical formation and the subsequent radical coupling.

Investigations of the products of decarboxylation and the factors that influence the decarboxylation of multicarboxylic acids are ongoing in our laboratory. We have found that high temperature and low pH are very effective for decarboxylation in the presence of *ds*-block metal ions.[2] Here, decarboxylation also occurs at high temperature and low pH in the presence of Tb(III) or Yb(III) ions. Thus, the study of decarboxylation factors can be supplemented and applied to some lanthanide ions such as Tb(III) and Yb(III) ions.

Metal−organic frameworks (MOFs) containing lanthanide (Ln) ions are attractive because of their versatile coordination chemistry, unique luminescent[17] and magnetic properties, and possible high framework stability. Guest-sensitive properties, such as the guest-dependent luminescence of lanthanide polymers, have become an interesting focus. However, to the best of our knowledge, few examples of the guest-dependent luminescent property of a lanthanide complex have been reported. In these studies, the luminescence of the complex decreases when the complex is dehydrated because the surrounding framework of the Tb^{3+} ion becomes soft.[18] In the present work, the luminescence intensity increases with the removal of water molecules, and the framework does not collapse when it is dehydrated. This phenomenon may have a certain value for the research and application of guest sensing and recognition because it can produce a luminescent response to guest absorption and exchange.[19]

Received: November 12, 2013
Published: June 30, 2014

Table 1. Crystal Data and Structure Refinement Information for Complexes 1 and 2

	complex 1	complex 2
formula	$C_{25}H_{22}N_3O_{28}Tb_3$	$C_{11}H_{25}NO_{24}Yb_2$
fw	1289.22	901.40
crystal system	monoclinic	triclinic
space group	$P2_1/c$	$P\bar{1}$
a (Å)	27.780(6)	8.6697(17)
b (Å)	6.6928(13)	10.155(2)
c (Å)	17.125(3)	13.455(3)
α (deg)	90	85.39(3)
β (deg)	92.90(3)	89.00(3)
γ (deg)	90	77.26(3)
V (Å^3)	3179.8(11)	1151.7(4)
Z	4	2
F (000)	2448	848
D_c (Mg m^{-3})	2.693	2.582
abs coeff (mm^{-1})	6.726	8.185
GoF on F^2	1.061	1.094
parameters	540	359
θ range (deg)	2.20−25.00	1.52−27.84
reflections collected/unique	16951/5372 [R(int) = 0.0424]	8446/5303 [R(int) = 0.0226]
reflections [$I > 2\sigma(I)$]	4638	4485
final R [$I > 2\sigma(I)$]	R_1 = 0.0420, R_2 = 0.0969	R_1 = 0.0376, R_2 = 0.0699
R indices (all data)	R_1 = 0.0494, R_2 = 0.1010	R_1 = 0.0475, R_2 = 0.0747
largest difference peak and hole (e Å^{-3})	4.310, −2.068	2.513, −1.575

Furthermore, the investigation of hydrogen-bonded water clusters or networks and the description of the morphology of water clusters with novel structure are also fascinating. It is exciting that large water clusters, novel water tapes, and water layers were recently observed and reported by our group.[2,20−23] In this work, a novel two-dimensional (2D) water layer containing T8(4)10(4) water tape as the substructure can provide insight into the hydrogen-bonding motif and the understanding of the 2D structure of water.

Herein, two new three-dimensional (3D) lanthanide coordination polymers from H_4ptc and its decarboxylation products, $\{[Tb_3(Hptc)(ptc)(pdc)(H_2O)_6]\cdot 2H_2O\}_n$ (**1**) and $\{[Yb_2(ptc)(ox)(H_2O)_5]\cdot 7H_2O\}_n$ (**2**), have been successfully synthesized and structurally characterized by single-crystal X-ray diffraction, element analysis, and IR, fluorescence, and thermal analyses. In **1**, Tb(III) ions are bridged by the carboxyl groups of the ligands, resulting in a three-dimensional (8,8)-connected net with a Schläfli symbol of $(3^3\cdot 4^{18}\cdot 5^5\cdot 6^2)_2(3^6\cdot 4^{14}\cdot 5^7\cdot 6)$. In **2**, the Yb(III) framework is bridged by the carboxyl groups of ptc^{4-} and ox^{2-}, forming an usual (4,8)-connected **sqc21** net with a Schläfli symbol of $(3^2\cdot 4^2\cdot 5^2)(3^4\cdot 4^8\cdot 5^{12}\cdot 6^4)$.

EXPERIMENTAL SECTION

Materials and Measurements. Potassium pyridine-2,3,5,6-tetracarboxylic acid (K_4ptc) was synthesized according to literature.[20] H_4ptc was prepared by acidizing K_4ptc with hydrochloric acid. Other chemicals were reagent grade and used without further purification. Elemental analyses for C, H, and N were performed on a PerkinElmer 240 CHN elemental analyzer. IR spectra were recorded in the range of 400−4000 cm^{-1} with a Bruker TENOR 27 spectrophotometer using a KBr pellet. Thermogravimetric analysis (TGA) experiments were performed on NETZSCH STA 409 PC/PG and PTC-10A TG-DTA instruments with a heating rate of 10 °C min^{-1}. Photoluminescence spectra were measured by an F-4500 FL spectrophotometer with a xenon arc lamp as the light source.

Preparation of $\{[Tb_3(Hptc)(ptc)(pdc)(H_2O)_6]\cdot 2H_2O\}_n$ (1). A mixture of Tb_4O_7 (0.0280 g, 0.0375 mmol), H_4ptc (0.0383 g, 0.15 mmol), HCl (0.5 mL, 2 mol L^{-1}), and water (10 mL) was poured into a 25 mL Teflon high-temperature kettle and kept at 150 °C for 24 h. Then it was cooled to 110 °C at a rate of 2 °C h^{-1} and to room temperature at a rate of 1 °C h^{-1}. The pH value of the solution was about 2. Crystals of **1** were obtained. Yield 52% based on Tb. Anal. Found: C, 23.56; H, 1.89; N, 3.65%. Calcd for $C_{25}H_{22}N_3O_{28}Tb_3$ (fw = 1289.22): C, 23.29; H, 1.71; N, 3.26%. IR (KBr, cm^{-1}): ν = 3423s, 1705w, 1600s, 1455s, 1362s, 1336s, 1161s, 887w, 672m.

Preparation of $\{[Yb_2(ptc)(ox)(H_2O)_5]\cdot 7H_2O\}_n$ (2). A mixture of $Yb(NO_3)_3\cdot 6H_2O$ (0.0934 g, 0.2 mmol), H_4ptc (0.0510 g, 0.2 mmol), and water (10 mL) was poured into a 25 mL Teflon high-temperature kettle and kept at 150 °C for 24 h. Then it was cooled to 110 °C at a rate of 2 °C h^{-1} and to room temperature at a rate of 1 °C h^{-1} The pH value of the solution was 2−3. Colorless crystals of **2** were obtained. Yield 47% based on Yb. Anal. Found: C, 14.76; H, 2.80; N, 1.55%. Calcd for $C_{11}H_{25}NO_{24}Yb_2$ (fw = 901.40): C, 14.66; H, 2.77; N, 1.55%. IR (KBr, cm^{-1}): ν = 3429s, 1662vs, 1422s, 1318s, 1149s, 887w, 821w, 634m.

Crystal Structure Determinations. Single-crystal X-ray diffraction data of **1** and **2** were collected on a computer-controlled Rigaku Saturn CCD area detector diffractometer equipped with confocal monochromatized Mo Kα radiation with a radiation wavelength of 0.71073 Å using the $\omega-\varphi$ scan technique. The structures were solved by direct methods and refined with a full-matrix least-squares technique based on F^2 using the SHELXS-97 and SHELXL-97 programs.[24] Anisotropic thermal parameters were assigned to all non-hydrogen atoms. Crystallographic data and structural refinement parameters are listed in Table 1.

RESULTS AND DISCUSSION

Syntheses of 1 and 2. A hydrothermal reaction of Tb_4O_7 with H_4ptc in water in the presence of HCl results in the formation of **1**, while a reaction of $Yb(NO_3)_3$ with H_4ptc in water leads to the formation of **2**. In complex **1**, pdc^{2-} might form from the ptc^{4-} through the cleavage of the C−C bond and the release of CO_2 molecules, while in complex **2**, oxalate may form from the coupling of two $^{\cdot}CO_2^-$ radicals released from ptc^{4-}.

The decarboxylation behavior has been clearly observed for some ligands similar to H_4ptc, such as pyrazine-2,3,5,6-

dx.doi.org/10.1021/ic402803s | Inorg. Chem. 2014, 53, 7092−7100

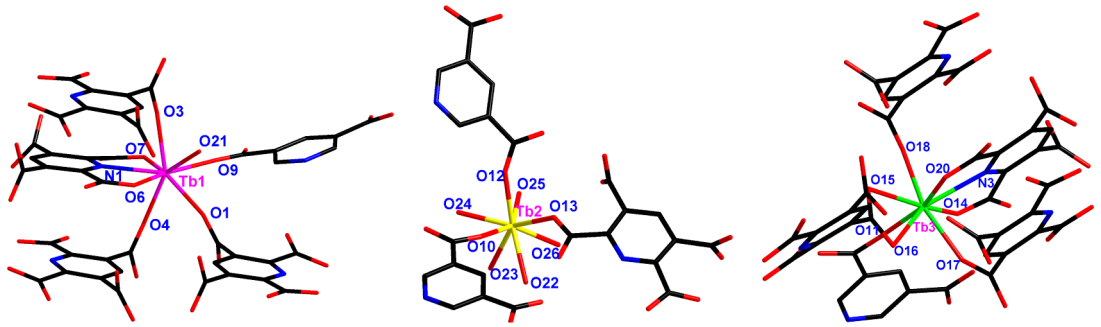

Figure 1. Coordination environments of Tb1, Tb2, and Tb3 in **1**, which are shown in purple, yellow, and green, respectively. H atoms are not shown for clarity.

tetracarboxylic acid (H_4pztc). In our previous work,[2] a series of hydrothermal reactions of H_4pztc were designed to explore the effect of temperature and pH on the decarboxylation of H_4pztc. The results showed that decarboxylation of H_4pztc occurred more easily at high temperature and low pH. Because the two ligands have very similar structures, for example, both belong to the N-heterocyclic ligands containing four carboxyl groups, it was inferred that decarboxylation also occurred at high temperature and low pH in the presence of Tb(III) or Yb(III) ions because the reactions were carried out under the conditions of low pH (about 2−3) and high temperature (150 °C). Then complexes **1** and **2** have the distinct 3D open-framework architectures due to the presence of pdc^{2-} and ox^{2-}, respectively.

Structural Analyses of $\{[Tb_3(Hptc)(ptc)(pdc)(H_2O)_6]\cdot 2H_2O\}_n$ (1). Complex **1** crystallizes in the monoclinic system in the $P2_1/c$ space group. Complex **1** is a very uncommon complex because it shows the following three characteristics: (1) the metal ions have three coordination modes, and Tb1 and Tb3 are coordinated by five multicarboxylate ligands to overcome the steric hindrance; (2) two crystallographically independent coordination modes ($Hptc^{3-}$ and ptc^{4-}) of the ligand are shown, which are reported for the first time; and (3) decarboxylation occurred during the synthesis under high temperature and low pH, and 3,5-bipyridine carboxylate (pdc^{2-}) was obtained.

Complex **1** is a 3D open MOF constructed via $Hptc^{3-}$, ptc^{4-}, pdc^{2-}, and Tb(III) ions. The asymmetric unit of **1** consists of three crystallographically independent Tb(III) atoms, one $Hptc^{3-}$, one ptc^{4-}, one pdc^{2-}, six coordinated water molecules, and two uncoordinated water molecules, in which Tb1, Tb2, and Tb3 are all 8-coordinated and adopt square antiprismatic geometries. Especially, for Tb1 and Tb3, they are very rare examples for five multicarboxylate ligands coordinating to one metal center.[25] The coordination environments of Tb1, Tb2, and Tb3 are shown in Figure 1.

Each Tb1 ion coordinates with one tridentate $Hptc^{3-}$ (O6, O7, and N1) and three monodentate $Hptc^{3-}$ (O3, O4, and O1) together with one monodentate pdc^{2-} (O9) and a coordinated water molecule (O21). Tb2 is coordinated by eight O atoms, three of which are from carboxylate groups of one ptc^{4-} (O13) and two pdc^{2-} (O10 and O12), and the other five are from water molecules. Each Tb3 ion also coordinates with five multicarboxylate ligands: one tridentate ptc^{4-} (O14, N3, and O20), one bidentate ptc^{4-} (O15 and O16), two monodentate ptc^{4-} (O17 and O18), and one monodentate pdc^{2-} (O11). The average $Tb-O_{carboxylate}$, $Tb-O_{water}$, and Tb−N bond lengths are shown in Table 2. The average Tb−O and Tb−N bonds lengths for Tb1 and Tb3 are obviously shorter than those documented in the literature,[26] which may be because the five multicarboxylate ligands coordinating with one metal center made the structures more compact. The formation of these coordination structures overcomes the steric hindrance.

Table 2. Coordination Numbers (CN) and Average Bond Lengths (Å) in Complexes 1 and 2

complex	metal ion	CN	$Ln-O_{carboxylate}$	$Ln-O_{water}$	Ln−N
1	Tb1	8	2.360	2.415	2.500
	Tb2	8	2.362	2.412	
	Tb3	8	2.366		2.510
2	Yb1	9	2.419	2.286	2.429
	Yb2	8	2.299	2.346	

In complex **1**, H_4ptc has not been completely deprotonated, and it forms $Hptc^{3-}$ and ptc^{4-}, two different anions with two different coordination modes (Figure 2), both of which are found for the first time. $Hptc^{3-}$ coordinates four Tb1 ions with monodentate, bidentate, and tridentate modes (Figure 2, mode A), while ptc^{4-} coodinates four Tb3 and one Tb2 with monodentate, bidentate, and tridentate modes (Figure 2, mode B). For pdc^{2-}, it coordinates one Tb1, one Tb3, and two Tb2 ions with bidentate modes, and the N ion does not coordinate to any metal ion (Figure 2, mode C).

Then, Tb1 ions are bridged by $Hptc^{3-}$ (Figure 2, mode A) to form a sort of layer structure in the *bc* plane (Figure 3). Each $Hptc^{3-}$ acts as bridging ligand and bridges four Tb1 ions: the head side of the ligand coordinates one Tb1 in a tridentate manner, and the tail side bridges three Tb1 centers in monodentate and bidentate manners. Each Tb1 ion is also coordinated by four $Hptc^{3-}$ from its four directions. Simultaneously, each Tb1 center is coordinated by one carboxylate O atom (O9) from pdc^{2-}, which sticks off the layer structure so that the layer can further self-assemble into a 3D structure.

Similarly, Tb3 ions are bridged by ptc^{4-} (Figure 2, mode B) to form another sort of layer structure also in the *bc* plane (Figure 4). The layer has some similarities with the one previously discussed: ptc^{4-} coordinates four Tb3 ions, and each Tb3 ion is connected by four ptc^{4-} ligands. However, there are some differences: each ptc^{4-} also coordinates one Tb2 ion, except four Tb3 ions, and Tb3 is also coordinated by one pdc^{2-}, which makes the layer connect on the outside and form the 3D network.

Furthermore, the Tb2 ion is coordinated by three carboxylate O atoms from ptc^{4-} and pdc^{2-} and five water molecules to form an infinite asymmetric chain along the *c* axis (Figure 5). The other carboxylate O atoms from ptc^{4-} and pdc^{2-} coordinate

dx.doi.org/10.1021/ic402803s | Inorg. Chem. 2014, 53, 7092−7100

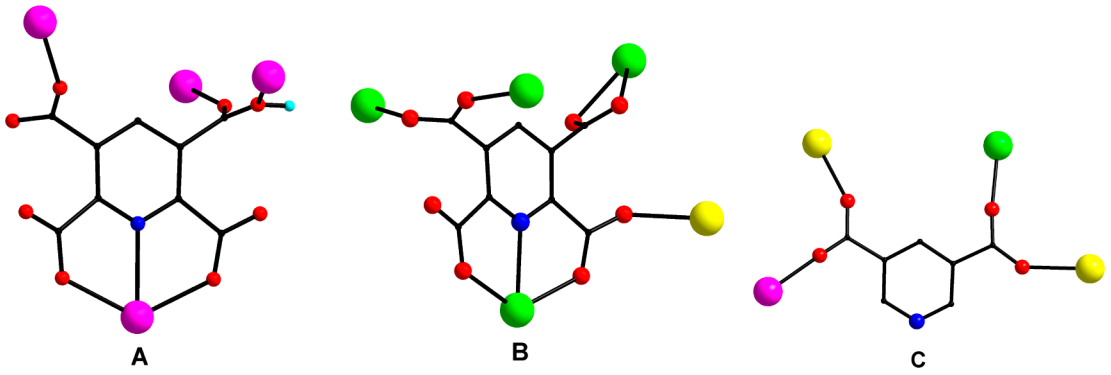

Figure 2. Coordination modes for (A) $Hptc^{3-}$, (B) ptc^{4-}, and (C) pdc^{2-} in **1**.

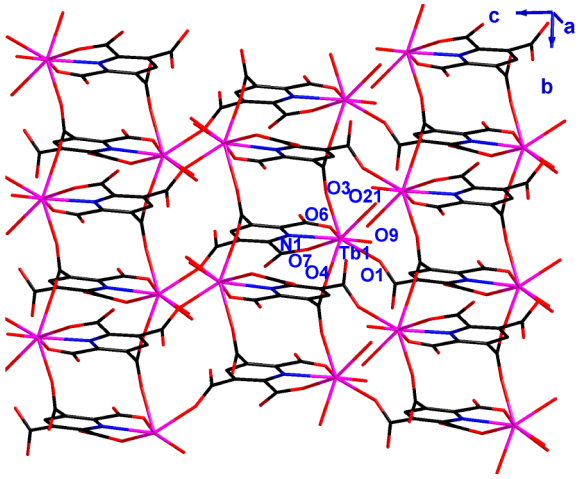

Figure 3. Layer structure formed by Tb1 and $Hptc^{3-}$ (Figure 2, mode A) in **1**. H atoms are not shown for clarity.

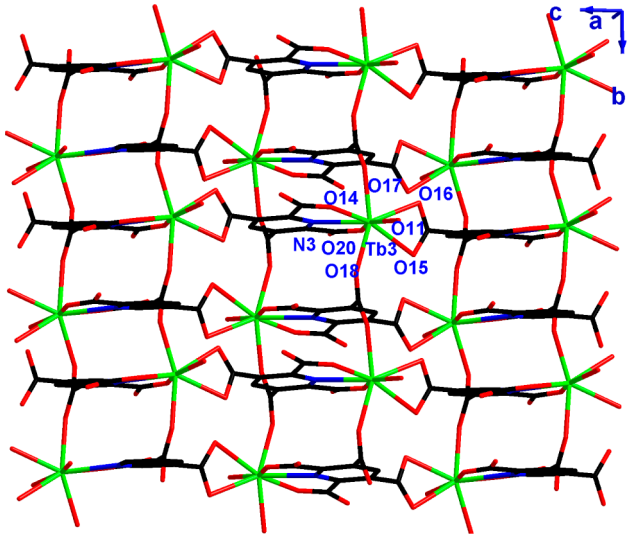

Figure 4. Layer structure formed by Tb3 and ptc^{4-} (Figure 2, mode B) in **1**.

Tb1 and Tb3 ions, which makes the chain connect with the two layer structures described above. The connection of the three kinds of Tb ions is shown in Figure 6.

Two types of layer structures are connected by a chain structure to form 3D coordination networks (Figure 7). When viewed along the *b* or *c* axis, the two layer structures present

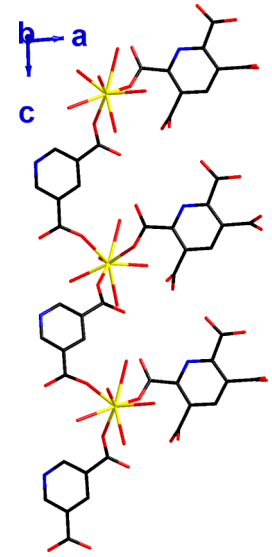

Figure 5. Infinite asymmetric chain formed by Tb2 and pdc^{2-} in **1**.

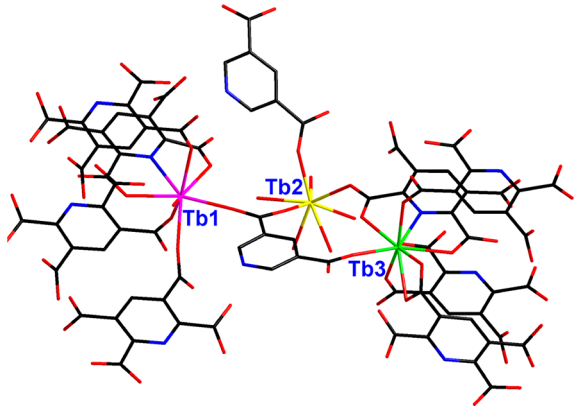

Figure 6. Connection of the Tb1, Tb2, and Tb3 ions in **1**.

themselves alternately, and the chain formed by Tb2, ptc^{4-}, and pdc^{2-} interspaces the two layers, which acts as the connector to help form the 3D network. It seems that Tb2 ions and pdc^{2-} play an important role in the formation of the 3D network.

Furthermore, the rich hydrogen-bonding network involving the water molecules, the carboxylate oxygen atoms, and the aromatic N atom of pdc^{2-} inserts in the framework of complex, which makes the 3D structure more rigid and steady.

Structural Analyses of $\{[Yb_2(ptc)(ox)(H_2O)_5]\cdot 7H_2O\}_n$ (2). Complex **2** crystallizes in the triclinic system in the $P\bar{1}$ space

dx.doi.org/10.1021/ic402803s | *Inorg. Chem.* 2014, 53, 7092−7100

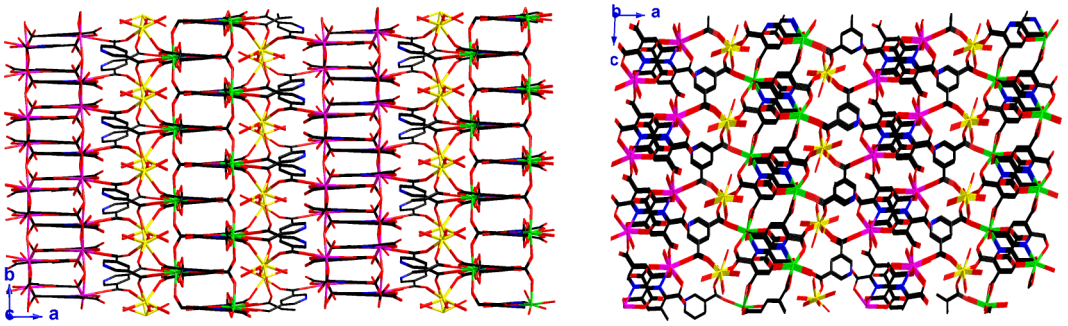

Figure 7. Two-layer structures connected by chain structures to form 3D coordination networks viewed along (left) the *c* axis and (right) the *b* axis in **1**.

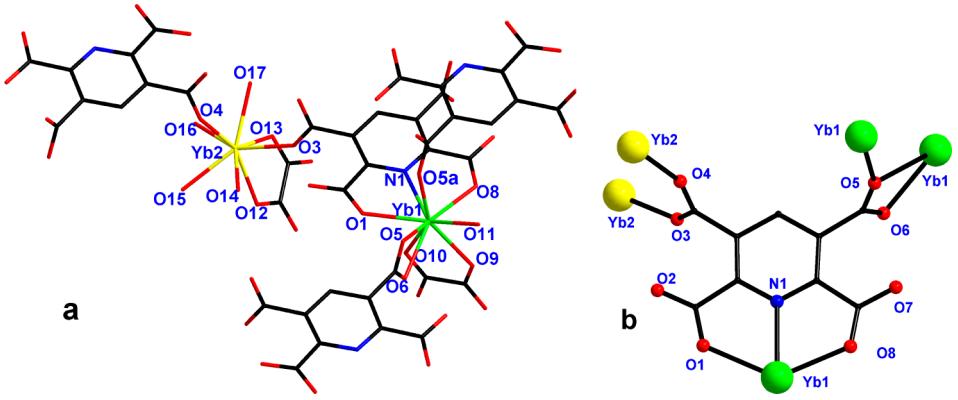

Figure 8. (a) Coordination environments of Yb1 and Yb2, which are shown in green and yellow, respectively. (b) Coordination mode for ptc^{4-} in **2**.

group. Complex **2** shows the following two characteristics: (1) decarboxylation occurs during the synthesis under high temperature and low pH, and oxalate is obtained from the coupling of two $^{\cdot}CO_2^-$ radicals, similar to the process that also occurred in other systems;[16] (2) a novel water layer is observed in **2**, which is novel in the Cambridge Structural Database (CSD).[27]

Complex **2** is a 3D open MOF constructed by Yb1, Yb2, ptc^{4-}, and ox^{2-}. The asymmetric unit of **2** consists of two crystallographically independent Yb(III) atoms, one ptc^{4-}, one ox^{2-}, five coordinated water molecules and six and three-quarters uncoordinated water molecules (Figure 8a). Yb1 is 9-coordinated with monocapped square antiprism coordination geometry, and Yb2 is 8-coordinated with distorted square antiprism coordination geometry. Yb1 ion is coordinated by one tridentate ptc^{4-} (O1, N1, and O8), bidentate ptc^{4-} (O5 and O6), and ox^{2-} (O9 and O10), together with one monodentate ptc^{4-} (O5a) and one coordinated water molecule (O11). Yb2 is coordinated by four coordinated water molecules (O14, O15, O16, and O17) and four carboxylate O atoms, of which two are from two ptc^{4-} in monodentate mode (O3 and O4) and two are from one ox^{2-} (O12 and O13) in bidentate chelating mode. The average Yb−$O_{carboxylate}$, Yb−O_{water}, and Yb−N bond lengths are shown in Table 2. The Yb1−$O_{carboxylate}$ bond lengths are obviously longer than Yb2−$O_{carboxylate}$ bond lengths because of the existence of a longer Yb(1)−O(5) bond with a bond length of 2.890 Å and the increase in the coordination number.

In complex **2**, ptc^{4-} adopts a different coordination mode with **1** (Figure 8b), which is reported first. H_4ptc is completely deprotonated in complex **2**, which coordinates to three Yb1 ions with a tridentate mode and two Yb2 with a bidentate mode.

As shown in Figure 9, two Yb1 ions (Yb1 and Yb1a) are linked by O5 and O5′ atoms to form a binuclear unit, and every

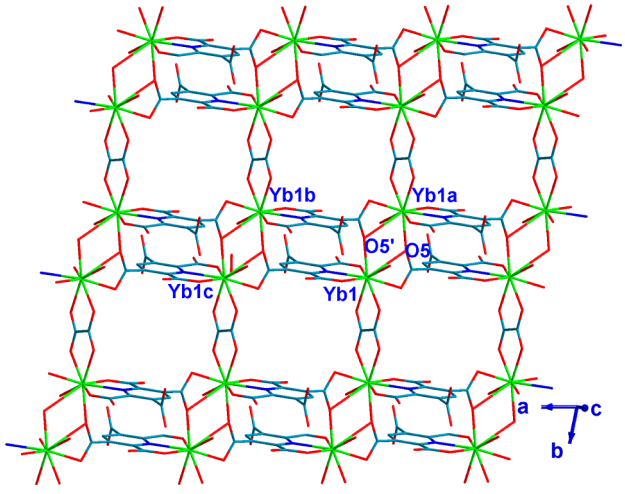

Figure 9. Infinite 2D structure formed by Yb1 ions and bridging ligands in **2**.

two units continue to be bridged by two ptc^{4-} to form a double chain structure along the *a* axis. Then ox^{2-} ligands act as connectors to link the double-chains and form an infinite 2D structure in the *ab* layer. All Yb1 ions in the 2D structure are coplanar, and the four Yb1 ions link together to form a parallelogram building block with distances of 4.458 Å

dx.doi.org/10.1021/ic402803s | *Inorg. Chem.* 2014, 53, 7092−7100

(between Yb1 and Yb1a) and 8.670 Å (between Yb1 and Yb1c).

As shown in Figure 10, two Yb2 ions are connected to two ptc^{4-} in a bidentate coordinating mode to form eight-numbered

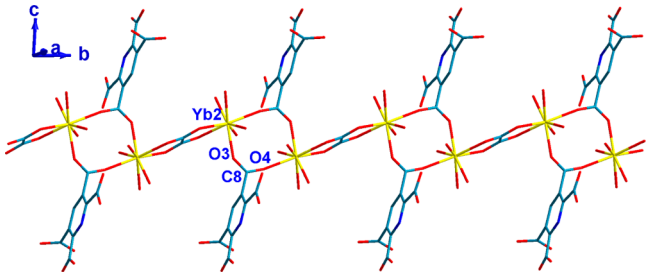

Figure 10. Infinite 1D structure formed by Yb2 ions and bridging ligands in **2**.

rings (Yb2, O3, O4, and C8 and their symmetric equivalents), which are further connected by ox^{2-} to form a 1D chain along the *b* axis. The other three carboxylate groups of ptc^{4-} ligands coordinate to Yb1 ions, which makes the chain connect with the above layer structure. Thus, the infinite one-dimensional (1D) chain acts as the connector to connect the layer structure to form the 3D coordination network. When viewed along the *a* or *b* direction (Figure 11), the 3D network is seen to be formed by a 2D layer structure formed by Yb1 ions in the *ab* layer and an infinite chain structure formed by Yb2 ions along the *b* axis.

The simplified topological structures of **1** and **2** can be finished by the application of topology analysis via the freely available computer program TOPOS.[28] As depicted in Figure 12, for **1**, if the binuclear Tb1Tb2(pdc) clusters are viewed as 8-connected nodes and the Tb3(ptc) clusters are viewed as 8-connected nodes, then the structure can be described as a usual (8,8)-connected net with a Schläfli symbol of $(3^3{\cdot}4^{18}{\cdot}5^5{\cdot}6^2)_2(3^6{\cdot}4^{14}{\cdot}5^7{\cdot}6)$. Topologically, for **2**, if the binuclear $Yb2_2(OX)$ clusters are considered as 4-connected nodes and $Yb1_2(ptc)$ clusters are viewed as 8-connected nodes, then the structure can be simplified as a (4,8)-connected **sqc21** net with a Schläfli symbol of $(3^2{\cdot}4^2{\cdot}5^2)(3^4{\cdot}4^8{\cdot}5^{12}{\cdot}6^4)$, which is rare for 3D MOFs.

A novel 2D water layer is stabilized in the 3D network (Figure 13a). The 2D water layer is basically an assembly of T8(4)10(4)[29] water tapes that are interconnected via O19···O20 and O17···O20 hydrogen bonds (Figure 13b). The

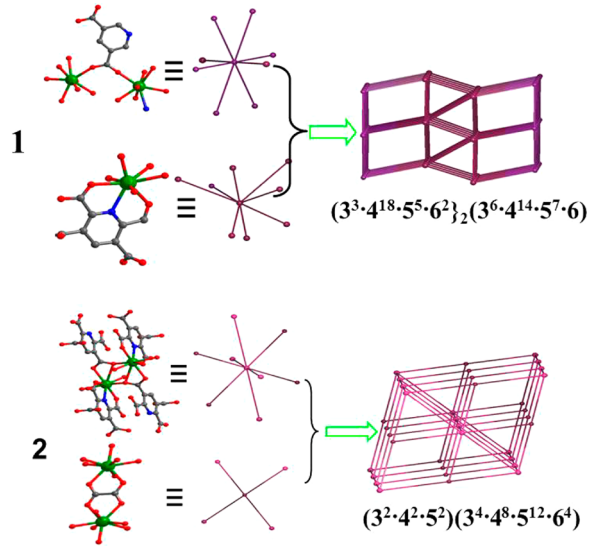

Figure 12. Schematic representation of the (8,8)-connected 3D net with a Schläfli symbol of $(3^3{\cdot}4^{18}{\cdot}5^5{\cdot}6^2)_2(3^6{\cdot}4^{14}{\cdot}5^7{\cdot}6)$ for **1** and (4,8)-connected **sqc21** net with a Schläfli symbol of $(3^2{\cdot}4^2{\cdot}5^2)(3^4{\cdot}4^8{\cdot}5^{12}{\cdot}6^4)$ for **2**.

T8(4)10(4) water tape as the substructure of the water layer is described in detail (Figure S1a in Supporting Information). The water molecules form 8-membered and 10-membered cyclic rings, in which four water molecules (O24, O17, O14, and O15) are shared to form an extended tape along the *a* axis. On the two sides of the tape, every water molecule hydrogen-bonds to one water molecule, and the hydrogen-bonding motif of the water tape presented herein is multiplied. O16 and O15 act as acceptors or donors to form three and four hydrogen bonds, respectively. In O24 (Figure S1b in Supporting Information), an 8-centered (pentafurcate) hydrogen bond is formed. O24 acts as a donor to hydrogen-bond two water molecules (O11 and O15) and as an acceptor to be hydrogen-bonded by three water molecules (O16, O17, and O18). To the best of our knowledge, the formation of this type of hydrogen bond around one water molecule is very difficult to form because of the steric hindrance.[20,21]

Furthermore, lattice water molecule O20 does not participate in this water tape; instead, it is inserted in the space between two tapes and acts as the connector to link two tapes into a 2D water layer through O19···O20 and O17···O20 hydrogen bonds

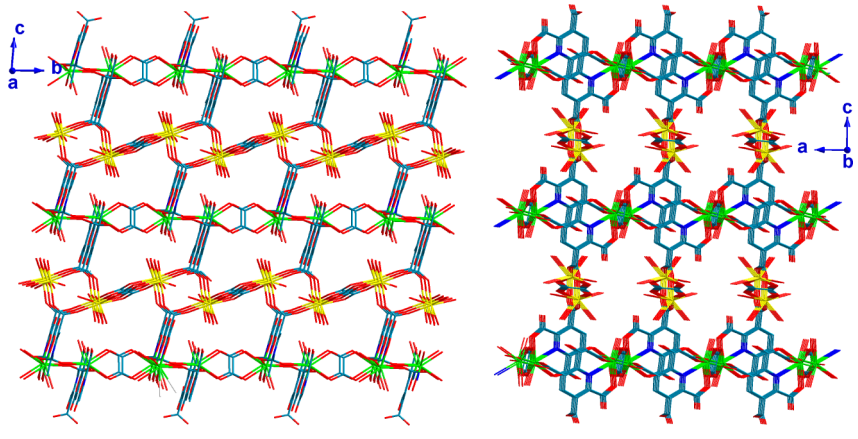

Figure 11. 3D structure of **2** when viewed along (left) the *a* axis and (right) the *b* axis.

dx.doi.org/10.1021/ic402803s | *Inorg. Chem.* 2014, 53, 7092−7100

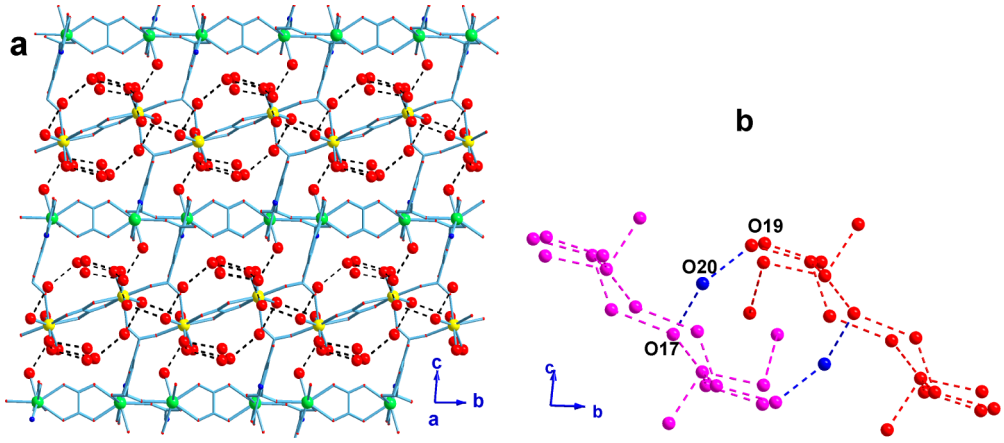

Figure 13. (a) Interactions between the water clusters and the complex framework. (b) Water layer viewed along the *a* axis in **2**. Hydrogen atoms are omitted for clarity.

(Figure S2 in Supporting Information). Thus, an infinite water layer is formed through numerous O20 connections in the interspaces of a complex framework.

Nonbonded O···O distances and O−H···O angles for the cluster are presented in Table 3. The O···O distances range from 2.707 to 3.470 Å, resulting in an average O···O distance of 2.949 Å. The O···O···O angles range from 126.69 to 170.89°, and the average O···O···O angle is 149.57°. We believe that this type of water cluster structure has not been described previously.

Table 3. Hydrogen Bond Data (Å, deg) in 2

D−H···A[a]	*d*(D−H)	*d*(H···A)	*d*(D···A)	∠(DHA)
O11−H11A···O24[b]	0. 850	1.969	2.766	155.69
O14−H14B···O17[c]	0.850	2.433	3.019	126.69
O14−H14B···O21′d[c]	0.850	2.635	3.470	167.72
O15−H2B···O24[d]	0.850	2.357	3.141	153.71
O16−H16A···O23[e]	0.850	1.938	2.707	149.94
O17−H17A···O20a	0.850	2.278	3.021	146.14
O17−H17B···O14[c]	0.850	2.386	3.019	131.63
O18−H18A··· O23	0.857	1.932	2.713	150.93
O19−H19B···O20′b[f]	0.850	2.288	2.892	128.24
O23−H23A···O19	0.850	1.977	2.795	161.26
O23−H23B···O22	0.850	1.874	2.717	170.89
O24−H24A···O16[c]	0.850	2.378	2.968	127.02
O24−H24A···O17[c]	0.850	2.397	3.214	161.23
O24−H24B···O18[g]	0.850	2.025	2.848	162.95

[a]D = donor; A = acceptor. [b]Symmetry code: −*x*, −*y*, −*z* + 1. [c]Symmetry code: −*x* + 1, −*y*, −*z*. [d]Symmetry code: −*x*, −*y*, −*z*. [e]Symmetry code: −*x* + 1, −*y* + 1, −*z*. [f]Symmetry code: *x* + 1, *y*, *z*. [g]Symmetry code: *x*, *y* − 1, *z*.

TGA. TGA was carried out for **1** in the as-prepared phase in the temperature range of 30−700 °C (Figure S3A in Supporting Information). The first weight loss from 70 to 110 °C is 3.30%, corresponding to the loss of two uncoordinated water molecules (calcd 2.79%). The second weight loss, 8.94%, occurred in the temperature range of 110−150 °C due to the loss of six coordinated water molecules (calcd 8.38%). The third weight loss above 460 °C corresponds to the decomposition of the compound.

Luminescence of the Complex upon Anhydrous and Enhydrous Phases. To investigate the effect of the water molecules on the framework and the luminescence intensity, the luminescence measurements of samples containing different water molecules were studied. Powder X-ray diffraction (PXRD) and TGA were used to check the phases. The as-prepared sample (A) was heated at 130 °C for 1 h, leading to loss of two uncoordinated water molecules, as evidenced by TGA (Figure S3 in Supporting Information), where the weight loss of 9.1% up to 150 °C corresponds to the loss of six water molecules (calcd 8.62%). Thus, a sample loss of two water molecules (B) was obtained. The as-prepared sample (A) was heated at 250 °C for 7 h, leading to a loss of eight water molecules and yielding sample C, which was also checked by TGA.

The luminescent property of **1** upon anhydrous and enhydrous phases is shown in Figure 14. For A, the excitation wavelength for the emission spectra is 340 nm. The excitation slit and the emission slit are 10 and 5 nm, respectively. The fluorescent emission consists of four main peaks at 495 ($^5D_4 \rightarrow {}^7F_6$), 549 ($^5D_4 \rightarrow {}^7F_5$), 586 ($^5D_4 \rightarrow {}^7F_4$), and 622 nm ($^5D_4 \rightarrow {}^7F_3$). The emission band at 549 nm ($^5D_4 \rightarrow {}^7F_5$) is obviously stronger than the others. The fluorescent spectra show the characteristic peaks of the terbium complex.[30] However, for the partly or completely dehydrated samples (B and C), luminescence intensity increases so significantly that the

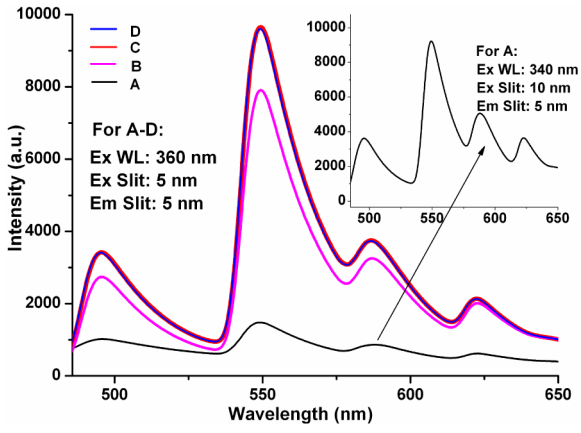

Figure 14. Emission spectra of **1** in its dehydrated and enhydrous phases: A, the sample as-prepared; B, the sample after the loss of two uncoordinated water molecules; C, the sample after the loss of eight water molecules; and D, the sample soaked in water for 24 h.

dx.doi.org/10.1021/ic402803s | *Inorg. Chem.* 2014, 53, 7092−7100

peaks overrun the measurement area. To compare the luminescence intensity more equitably for A–D, we chose the same instrumental conditions, an excitation wavelength of 360 nm, and both excitation and emission slits of 5 nm. It is interesting to observe the large intensity increase in luminescence upon dehydration of the sample. For B, the luminescence intensity is more than 5 times stronger than that of A on the strongest emission of the $^5D_4 \rightarrow {}^7F_5$ transition at 549 nm. When B continued to lose residual water molecules (C), the luminescence intensity continues to increase, while the peaks do not move. So, it is found that a decrease in the number of water molecules in samples is accompanied by an increase in luminescence intensity, which is accordant with terbium sulfate hydrate reported by Mamykin et al.,[31] but it is different from the Tb^{3+} complex reported by Gao et al.[18] in which a decrease of luminescence when it is dehydrated might relate to the amorphous feature of the dehydrated phases, where the surrounding of Tb^{3+} ion becomes soft.

In this work, the loss of two uncoordinated water molecules does not change the framework of the complex, so its perfect crystallinity can be preserved, as indicated by comparing their PXRD patterns to the as-prepared ones (Figure 15).

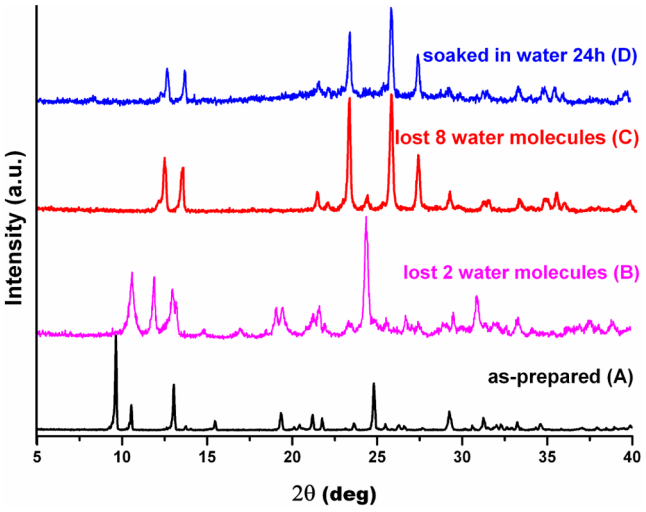

Figure 15. Powder X-ray diffraction patterns of dehydrated and enhydrous phases of **1**.

Furthermore, the decrease in the number of waters may reduce energy consumption caused by O–H vibrations in water molecules, which results in an increase in luminescence intensity. For C, the dehydrated phases showed X-ray scattering ability and obvious PXRD peaks, which indicated that the framework did not collapse, although some degradation might occur, and its luminescence intensity is stronger than that of B. Therefore, water molecules in fact weaken the luminescence but do not increase it when the framework has not collapsed.

When C was soaked in water for 24 h, sample D was obtained, the water molecules were not recovered, and its TGA and PXRD patterns, as well as its luminescence intensity, were similar to those of the dehydrated samples C. Thus, the dehydrated and rehydrated processes were not basically reversible for complex **1**.

CONCLUSION

In summary, we have demonstrated two 3D lanthanide coordination polymers of Tb(III) and Yb(III) obtained by the hydrothermal method of in situ decarboxylation. The decarboxylation products are pyridine-3,5-dicarboxylate and oxalate in **1** and **2**, respectively, which participate in coordination and play an important role in the formation of the 3D networks. The decarboxylation occurred under high temperature and low pH. For complex **1**, the luminescence intensity increases when the water molecules are driven off, and when the dehydrated sample is soaked in water, the water molecules cannot be recovered. The significant luminescence changes with different numbers of waters render the material potentially applicable for sensing water. For complex **2**, the novel 2D water layer containing T8(4)10(4) water tape as the substructure may provide insight into the hydrogen-bonding motif and enhance our understanding of the 2D structural aspects of water.

ASSOCIATED CONTENT

Supporting Information

Water tape substructure for **2**, TG curves for **1**, and crystallographic data for **1** and **2** (cif). This material is available free of charge via the Internet at http://pubs.acs.org. CCDC (781861-**1**, 770816-**2**) retains the supplementary crystallographic data for this work, which can be obtained free of charge via www.ccdc.can.ac.uk/conts/retrieving.html (or from the Cambridge Crystallographic Data Centre, 12 Union Road, Cambridge CB21EZ, UK; fax: (+44) 1223–336–033; or deposit@ccdc.cam.ac.uk).

AUTHOR INFORMATION

Corresponding Authors

*E-mail: cuijianzhong@tju.edu.cn. Fax: +86-22-27403475.
*E-mail: zhaobin@nankai.edu.cn

Notes

The authors declare no competing financial interest.

ACKNOWLEDGMENTS

This work was supported financially by the National Natural Science Foundation of China (Grants 21001078 and 21271137) and the Specialized Research Fund for the Doctoral Program of Higher Education (Grant 20121210120016).

REFERENCES

(1) (a) Min, K. S.; Suh, M. P. *J. Solid State Chem.* **2000**, *152*, 183–190. (b) Li, H.; Eddaoudi, M.; Groy, T. L.; Yaghi, O. M. *J. Am. Chem. Soc.* **1998**, *120*, 8571–8572. (c) Hill, C. L.; Zhang, X. *Nature* **1995**, *373*, 324–326. (d) Li, G.; Li, L.; Feng, S.; Wang, M.; Yao, X. *Adv. Mater.* **1999**, *11*, 146–149. (e) Zhao, C.; Feng, S.; Xu, R.; Shi, C.; Ni, J. *Chem. Commun.* **1997**, 945–946.

(2) (a) Tseng, T. W.; Luo, T. T.; Chen, S. Y.; Su, C. C.; Chi, K. M.; Lu, K. L. *Cryst. Growth Des.* **2013**, *13*, 510–517. (b) Knope, K. E.; Kimura, H.; Yasaka, Y.; Nakahara, M.; Andrews, M. B.; Cahill, C. L. *Inorg. Chem.* **2012**, *51*, 3883–3890. (c) Cai, S. L.; Zheng, S. R.; Wen, Z. Z.; Fan, J.; Wang, N.; Zhang, W. G. *Cryst. Growth Des.* **2012**, *12*, 4441–4449. (d) Li, Y.; Zou, W. Q.; Wu, M. F.; Lin, J. D.; Zheng, F. K.; Liu, Z. F.; Wang, S. H.; Guo, G. C.; Huang, J. S. *CrystEngComm* **2011**, *13*, 3868–3877. (e) Li, D. P.; Zhou, X. H.; Liang, X. Q.; Li, C. H.; Chen, C.; Liu, J.; You, X. Z. *Cryst. Growth Des.* **2010**, *10*, 2136–2145. (f) Zhong, D. C.; Lu, W. G.; Jiang, L.; Feng, X. L.; Lu, T. B. *Cryst. Growth Des.* **2010**, *10*, 739–746. (g) Yang, A. H.; Quan, Y. P.; Gao, H. L.; Fang, S. R.; Zhang, Y. P.; Zhao, L. H.; Cui, J. Z.; Wang, J. H.; Shi, W.; Cheng, P. *CrystEngComm* **2009**, *11*, 2719–2727. (h) Cheng, J. W.; Zheng, S. T.; Yang, G. Y. *Inorg. Chem.* **2008**, *47*, 4930–4935.

(3) Li, J.; Brill, T. B. *J. Phys. Chem. A* **2002**, *106*, 9491–9498.

(4) Li, X.; Cao, R.; Sun, D. F.; Shi, Q.; Bi, W. H.; Hong, M. C. *Inorg. Chem. Commun.* **2003**, *6*, 815−818.
(5) Yan, Y.; Wu, C. D.; Lu, C. Z. *Z. Anorg. Allg. Chem.* **2003**, *629*, 1991−1995.
(6) Zhang, X. M.; Fang, R. Q. *Inorg. Chem.* **2005**, *44*, 3955−3959.
(7) Zhang, X. M. *Coord. Chem. Rev.* **2005**, *249*, 1201−1219.
(8) Sun, Y. Q.; Zhang, J.; Yang, G. Y. *Chem. Commun.* **2006**, 1947−1949.
(9) Zheng, Y. Z.; Tong, M. L.; Chen, X. M. *J. Mol. Struct.* **2006**, *796*, 9−17.
(10) Li, M.; Xiang, J. F.; Yuan, L. J.; Wu, S. M.; Chen, S. P.; Sun, J. T. *Cryst. Growth Des.* **2006**, *6*, 2036−2040.
(11) Wu, W. P.; Wang, Y. Y.; Wu, Y. P.; Liu, J. Q.; Zeng, X. R.; Shi, Q. Z.; Peng, S. M. *CrystEngComm* **2007**, *9*, 753−757.
(12) Lisitsyn, A. S. *Appl. Catal., A* **2007**, *332*, 166−170.
(13) Gooßen, L. J.; Thiel, W. R.; Rodríguez, N.; Linder, C.; Melzer, B. *Adv. Synth. Catal.* **2007**, *349*, 2241−2246.
(14) Shepard, A. F.; Wilson, N. R.; Johnson, J. R. *J. Am. Chem. Soc.* **1930**, *52*, 2083−2090.
(15) (a) Han, Z. B.; Cheng, X. N.; Li, X. F.; Chen, X. M. *Z. Anorg. Allg. Chem.* **2005**, *631*, 937−942. (b) Qiong, Y. Q.; Yang, G. Y. *Dalton Trans.* **2007**, *34*, 3771−3781. (c) Huang, Y.; Song, Y. S.; Yan, B.; Shao, M. *J. Solid State Chem.* **2008**, *181*, 1731−1737. (d) Xie, C. Z.; Zhang, B. F.; Wang, X. Q.; Yu, B.; Wang, R. J.; Shen, G. Q.; Shen, D. Z. *Z. Anorg. Allg. Chem.* **2008**, *634*, 387−391.
(16) (a) Zhu, X. D.; Gao, S. Y.; Li, Y. F.; Yang, H. X.; Li, G. L.; Xua, B.; Cao, R. *J. Solid State Chem.* **2009**, *182*, 421−427. (b) Li, B.; Gu, W.; Zhang, L. Z.; Qu, J.; Ma, Z. P.; Liu, X.; Liao, D. Z. *Inorg. Chem.* **2006**, *45*, 10425−10427. (c) Min, D.; Lee, S. W. *Inorg. Chem. Commun.* **2002**, *5*, 978−983. (d) Li, X.; Cao, R.; Sun, D. F.; Shi, Q.; Bi, W. H.; Hong, M. C. *Inorg. Chem. Commun.* **2003**, *6*, 815−818. (e) Huh, H. S.; Lee, S. W. *Bull. Korean Chem. Soc.* **2006**, *27*, 1839−1843.
(17) (a) Hammell, J.; Buttarazzi, L.; Huang, C. H.; Morrow, J. R. *Inorg. Chem.* **2011**, *50*, 4857−4867. (b) Lin, Y. W.; Jian, B. R.; Huang, S. C.; Huang, C. H.; Hsu, K. F. *Inorg. Chem.* **2010**, *49*, 2316−2324. (c) Gu, J. Q.; Sun, L. D.; Yan, Z. G.; Yan, C. H. *Chem.—Asian J.* **2008**, *3*, 1857−1864. (d) Shen, L.; Shi, M.; Li, F. Y.; Zhang, D. Q.; Li, X. H.; Shi, E. X.; Yi, T.; Du, Y. K.; Huang, C. H. *Inorg. Chem.* **2006**, *45*, 6188−6197.
(18) Zhu, W. H.; Wang, Z. M.; Gao, S. *Inorg. Chem.* **2007**, *46*, 1337−1342.
(19) (a) Bai, Y.; He, G. J.; Zhao, Y. G.; Duan, C. Y.; Dang, D. B.; Meng, Q. J. *Chem. Commun.* **2006**, 1530−1532. (b) Mitchell-Koch, J. T.; Borovik, A. S. *Chem. Mater.* **2003**, *15*, 3490−3495.
(20) Yang, A. H.; Zhang, H.; Gao, H. L.; Zhang, W. Q.; He, L.; Cui, J. Z. *Cryst. Growth Des.* **2008**, *8*, 3354−3359.
(21) Quan, Y. P.; Zhao, L. H.; Yang, A. H.; Cui, J. Z.; Gao, H. L.; Lu, F. L.; Shi, W.; Cheng, P. *CrystEngComm* **2009**, *11*, 1679−1685.
(22) Zhao, L. H.; Quan, Y. P.; Yang, A. H.; Cui, J. Z.; Gao, H. L.; Lu, F. L.; Shi, W.; Cheng, P. *CrystEngComm* **2009**, *11*, 1427−1432.
(23) Yang, A. H.; Zhao, L. H.; Quan, Y. P.; Gao, H. L.; Cui, J. Z.; Shi, W.; Cheng, P. *Cryst. Growth Des.* **2010**, *10*, 218−223.
(24) (a) Sheldrick, G. M. *SHELXL-97 program for the solution of crystal structures*; University of Göttingen: Göttingen, Germany, 1997. (b) Sheldrick, G. M. *SHELXL-97 program for the refinement of crystal structures*; University of Göttingen: Göttingen, Germany, 1997.
(25) Gao, H. L.; Yi, L.; Ding, B.; Wang, H. S.; Cheng, P.; Liao, D. Z.; Yan, S. P. *Inorg. Chem.* **2006**, *45*, 481−483.
(26) Wang, H. S.; Zhao, B.; Zhai, B.; Shi, W.; Cheng, P.; Liao, D. Z.; Yan, S. P. *Cryst. Growth Des.* **2007**, *7*, 1851−1857.
(27) Mascal, M.; Infantes, L.; Chisholm, J. *Angew. Chem., Int. Ed.* **2006**, *45*, 32−36.
(28) Blatov, V. A.; Shevchenko, A. P.; Serezhkin, V. N. *J. Appl. Crystallogr.* **2000**, *33*, 1193; TOPOS software is available for download at http://www.topos.ssu.samara.ru.
(29) Infantes, L.; Chisholm, J.; Motherwell, S. *CrystEngComm* **2003**, *5*, 480−486.
(30) He, Z.; Gao, E. Q.; Wang, Z. M.; Yan, C. H.; Kurmoo, M. *Inorg. Chem.* **2005**, *44*, 862−874.
(31) Mamykin, A. A.; Mamykin, A. V.; Ostakhov, S. S.; Kazakov, V. P. *High Energy Chem.* **2010**, *44*, 109−112.